JOURNAL OF Materials CHEMISTRY

Enhanced hole injection in organic light-emitting diodes consisting of self-assembled monolayer of tripod-shaped π-conjugated thiols

Lihua Zhu,[a]† Heqing Tang,[b]† Yutaka Harima,‡*[a] Kazuo Yamashita,*[a] Yoshio Aso[b] and Tetsuo Otsubo[b]

[a]*Faculty of Integrated Arts and Sciences, Hiroshima University, Higashi-Hiroshima 739-8521, Japan. E-mail: harima@mls.ias.hiroshima-u.ac.jp; yamasita@mls.ias.hiroshima-u.ac.jp*
[b]*Graduate School of Engineering, Hiroshima University, Higashi-Hiroshima 739-8527, Japan*

Received 7th February 2002, Accepted 13th May 2002
First published as an Advance Article on the web 1st July 2002

Self-assembled monolayers (SAMs) of two tripod-shaped π-conjugated thiols and a disulfide have been grafted onto Au(111)/mica substrates. These SAMs exhibit oxidation and reduction peaks in the cyclic voltammograms arising from the electrochemical responses of the conjugated oligothiophene parts in the molecules. Organic light-emitting devices have been fabricated by using the SAM-coated Au electrode as the anode. In comparison with the device consisting of Au/TPD/Alq_3/Mg–Ag, the electroluminescence performance of the device using the SAM grafted Au electrode is much improved for the SAM of the tripod-shaped thiols and worsened for the SAM of the disulfide. The different influences of the SAMs on the performances are explained by considering structures of the molecules and the SAMs, and the energy level alignment at the related interfaces in the devices.

Introduction

Research on organic light-emitting diodes (OLEDs) has been attracting a lot of attention.[1] One of the elementary processes in OLEDs is charge transfer at the interface between an electrode and an organic molecular material. The dynamics of the heterogeneous charge (hole and electron) transfer depends on the energy barrier at the interface, which is determined by the difference between the work function of the electrode material and the energy of the highest occupied molecular orbital (HOMO) or the lowest unoccupied molecular orbital (LUMO) level of the organic molecular material. In a simple OLED composed of ITO/Alq_3/Al, where ITO and Alq_3, respectively, represent indium-doped tin oxide electrode and the well-known emitter tris(8-hydroxyquinolinato)aluminium(III), the energy barriers for the hole and electron injection are high up to about 1 eV. These charge injection barriers are required to be reduced for low operating voltage OLEDs. Using a metal with a smaller (or greater) work function as the cathode (or the anode) can result in a marked decrease in the operating voltage of the device. Alternatively, a hole transport layer (HTL) and/or electron transport layer (ETL) can be sandwiched between an electrode and the emitter layer in the fabrication of a low operating voltage OLED. One of the common HTLs is 4,4″-bis(3-methylphenyl-phenylamino)biphenyl (TPD), while Alq_3 is a good emissive ETL material. Metallophthalocyanines as HTLs have been found to reduce the operating voltages of Alq_3-type devices consisting of a TPD layer,[2–4] and a linear relationship has been found between the operating voltage of the device and the HOMO energy of the metallophthalocyanine.[3]

Self-assembled monolayers (SAMs) are ordered molecular assemblies that are formed spontaneously by the adsorption of organic molecules with a specific affinity of their head-groups to a substrate. The surface chemistry of the substrate can be modified significantly by the grafted SAM. The chemical versatility and unique characteristics of SAMs lead to their various potential technical applications in many fields such as model systems for surface chemistry, chemical sensors, protective coatings, mechanically modified coatings, non-linear optical devices, and OLEDs.[5] The fundamental aspects and potential applications of SAMs can be found in a recent review by Schreiber.[5] The utilization of SAMs in OLEDs and other molecular electronic devices are very possibly related to the fact that chemisorbed molecules lead to the generation of a dipole layer due to the charge transfer between the metal substrate and the chemisorbed species. The resulting dipole layer may enhance or hinder the moving of charge carriers, depending on the direction of orientation of dipoles. As a consequence, the work function of the metal is increased or decreased apparently, and the charge injection in OLEDs becomes tunable. Campbell and coworkers reported that the work function of modified Ag could be tuned over a range of 1 eV by using alkane-thiols.[6] Later, they demonstrated that the work function of Cu coated with the SAM of a conjugated-thiol ($HS–(C_6H_4C_2)_2C_6H_4–F$) was increased and the hole injection from Cu electrode to the polymer in Cu/polymer/Ca diodes was enhanced, whereas the SAM of another conjugated-thiol ($HS–(C_6H_4C_2)_2C_6H_4–H$) led to a decreased work function and depressed hole injection.[7] Nüesch *et al.* found that by grafting a SAM of nitrobenzoic acid onto ITO glass in a device ITO/Alq_3/Al, the current–voltage curve was shifted considerably to low voltage direction and the brightness was increased.[8] Appleyard and Willis reported that a SAM of 2-chloroethane phosphonic acid coated on ITO reduced the operating voltage of ITO/TPD/Alq_3/Al, and the reduction was very small for a device with Mg–Ag cathode instead of Al cathode.[9] Fujihira and co-workers demonstrated that characteristics of electroluminescent (EL) devices were improved dramatically by using ITO chemically modified with H-, Cl-, and CF_3-terminated benzoyl chlorides, and *p*-chlorobenzene derivatives with different binding groups of $-SO_2Cl$, -COCl, and $-PO_2Cl_2$.[10] It was found that an enormous increase in work function of the modified ITO up to 0.9 eV was possible using phenylphosphoryl dichloride with a CF_3-terminal group in the *para*-position.

The molecular design of self-assembling molecules makes SAMs more interesting in energy and charge transfer processes. For example, a multiple-point anchor in the molecule can

†Present address: Department of Chemistry, Huazhong University of Science and Technology, Wuhan, China.
‡Present address: Graduate School of Engineering, Hiroshima University, Higashi-Hiroshima 739-8527, Japan.

 DOI: 10.1039/b201391f

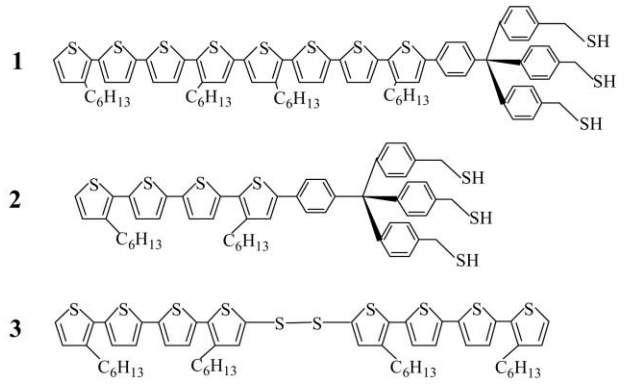

Fig. 1 Chemical structures of π-conjugated thiols **1**, **2** and disulfide **3**.

increase the chemical stability of the SAM. Embodying a large π-conjugated block in the molecule facilitates energy and charge transfer through the SAM. In a recent work,[11] we have preliminarily reported the cyclic voltammetry of a thiol with a three-point anchor and a π-conjugated quaterthiophene tail(**2** in Fig. 1) and its application to OLEDs. This SAM has been found to improve considerably the EL performances of Au/TPD/Alq_3/Mg–Ag devices. The influence of the SAM of this thiol on the EL performance of OLEDs are investigated in detail in this work. The role of this SAM in Au-SAM/TPD/Alq_3/Mg–Ag devices is further discussed by comparing with another tripod-shaped thiol with a longer π-conjugated octithiophene tail (**1**) and a quaterthiophene-containing disulfide (**3**).

Experimental

Compounds **1**, **2** and **3**, with chemical structures shown in Fig. 1, were synthesized chemically as described.[12] The head-groups were protected as acetylthiol groups, and deprotected just before grafting of the SAMs. Acetonitrile from Tokyo Kasei was refluxed over P_2O_5 for 2 hours under a nitrogen atmosphere and then distilled just before use. $LiClO_4$ from Aldrich was vacuum dried for 8 hours at 80 °C.

Semitransparent gold films of 30 nm thickness were electron beam deposited onto freshly cleaved mica at a deposition rate of 0.1 nm s^{-1}. The Au-coated mica sheets were annealed in an oven at 300 °C for 2 hours. The predominant atomic surface structure for the annealed Au/mica films obtained in our experiment was that of the (111) indexed plane as indicated by X-ray diffraction analysis.[13] SAMs were grafted onto the Au(111) substrates by immersing in deaerated dichloromethane solutions of compound **1**, **2** or **3** (1×10^{-4} mole dm^{-3}) for 20 hours or longer, followed by thoroughly rinsing with dichloromethane and then ethanol and finally by vacuum drying. The SAM-coated substrates were further vacuum deposited with a 60 nm thick TPD layer and a 60 nm thick Alq_3 layer and finally with a 200 nm thick top layer of Mg–Ag alloy at a deposition rate 0.3–0.5 nm s^{-1} at about 5×10^{-6} Torr. The light-emitting area of the device was 10×1 mm^2. For comparison, some other devices without any SAM were fabricated in a similar manner. Totally, five types of devices were prepared with configurations of Au-SAM **1**/TPD/Alq_3/Mg–Ag, Au-SAM **2**/TPD/Alq_3/Mg–Ag, Au-SAM **3**/TPD/Alq_3/Mg–Ag, Au/TPD/Alq_3/Mg–Ag, and ITO/TPD/Alq_3/Mg–Ag, which will be referred to as SAM(**1**), SAM(**2**), SAM(**3**), bare-Au, and bare-ITO devices hereafter, respectively. As described previously,[3] the EL characteristics were measured using a Takasago TP0120-06D regulated dc power supply, a Hokuto Denko HB-111 function generator, and a Hamamatsu H957-08 photomultiplier tube, which was calibrated with a Minolta LS-110 spot luminance meter. Cyclic voltammograms of the SAMs were conventionally measured in acetonitrile solution of 0.1 mol dm^{-3} $LiClO_4$. A Pt wire and an Ag/$AgClO_4$ (0.1 mol dm^{-3}) electrode were used as the counter and reference electrodes, respectively.

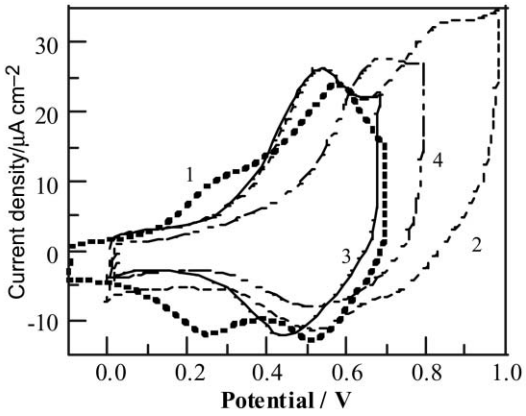

Fig. 2 Cyclic voltammograms of the Au(111) coated with (1) SAM **1**, (2) and (3) SAM **2** and (4) SAM **3** in acetonitrile solution containing 0.1 mole dm^{-3} $LiClO_4$. The difference between (2) and (3) was the upper potential limit as shown in the figure. The voltammograms were recorded in the first sweep at a sweep rate of 200 mV s^{-1}.

Results and discussion

Cyclic voltammetry

Cyclic voltammograms of the SAM-coated Au(111) measured at 200 mV s^{-1} in an acetonitrile solution of 0.1 mol dm^{-3} $LiClO_4$ are shown in Fig. 2. Two pairs of oxidation/reduction peaks are clearly seen at 0.27/0.25 V and 0.58/0.52 V for thiol **1**, and the cyclic voltammograms of **1** were found to be very stable during successive potential sweeping. This indicates an easy oxidation of this SAM due to a greater π-conjugated octithiophene unit in the molecule. The excellent electrochemical stability of this SAM is attributed to the low oxidation potential much below the potential at which the adsorbed thiol molecules would be anodically desorbed and to the stability of dications generated in the second-oxidation step of the π-conjugated octithiophene unit. In the case of thiol **2**, similarly, two pairs of anodic/cathodic peaks appear at 0.53/0.51 V and 0.86/0.72 V in the first cycle, corresponding to the oxidation and reduction of the π-conjugated quaterthiophene moiety in the molecules. Because of the smaller π-conjugated moiety, the second oxidation process was not so reversible, and the redox peaks became broader and decreased in current with the cycle number in this potential window. By reducing the upper potential limit to a value being less positive than about 0.7 V, however, the first reduction peak became sharper with a peak potential at 0.44 V and the cyclic voltammograms became quite stable during successive potential cycling, indicating that the one-electron oxidized stage of SAM **2** is quite stable. The tripod-shaped head-groups in the molecules of thiols **1** and **2** seem to play an important role in the good stability of SAMs **1** and **2**. In contrast, SAM **3** exhibits only one pair of oxidation/reduction peaks at 0.69/0.52 V in the first cycle of potential sweeping. The peak currents decreased rapidly in the second cycle and tended to disappear after several cycles of sweeping, indicative of a poor electrochemical stability of SAM **3**.

Integration of the anodic current over the potential window of the first oxidation peak in the first potential scan gave the surface coverage of the adsorbed molecules in the SAMs as 1.6×10^{-10}, 2.9×10^{-10}, and 1.3×10^{-10} mole cm^{-2} for **1**, **2** and **3**, respectively. These values of coverage are correspondingly equivalent to 4.8×10^{-10} mole cm^{-2} for **1**, 8.7×10^{-10} mole cm^{-2} for **2**, and 2.6×10^{-10} mole cm^{-2} for **3** in terms of the adsorbed sulfur atoms. The surface coverage values demonstrate that SAM **2** is compactly packed, because

the sulfur-atom surface coverage of **2** is comparable to the value of 9.3($\pm$0.6) $\times$ 10^{-10} mole cm^{-2} for compactly-packed SAMs of conventional alkylthiols on Au(111)/mica substrate.[13] In the case of **1**, the increased length of molecule and the increased number of hexyl substitutes (-C_6H_{13}) may account for the lesser compactness of SAM **1**. The sulfur-atom surface coverage of SAM **3** is only one-third of the value for compactly-packed SAMs of conventional alkylthiols on Au(111)/mica substrates. This is possibly related to the different conformation, *i.e.*, head group (–S–S–), and the rigidity of the π-conjugated tail in the molecule of **3**. A full interpretation needs further extensive work on the structural aspects of the SAMs.

The cyclic voltammetric behavior of SAMs **1** and **2** is similar to that observed for thiophene oligomers and oligothiophene-containing polymers dissolved in solution and in films: a two-step oxidation occurs, and the peak potentials decrease with increase of the thiophene ring number.[14] However, we noted the different cyclic voltammetric behaviors between SAMs **2** and **3**, which have the same π-conjugated quaterthiophene moiety. The potential of the first oxidation peak is 0.53 V for **2**, much lower than 0.69 V for **3**. These are attributed to two reasons at least. First, the orientation of molecules is different in these SAMs. The tripod-shaped head-groups of **2** make the molecules stand almost normal to the Au surface.[12] However, the normal standing of the quaterthiophene moieties becomes difficult in the case of **3**. Therefore, the quaterthiophene moieties in **3** become relatively difficult to be oxidized. Second, the quaterthiophene part is substituted by a benzene ring in **2**, leading to extension of the π-conjugation of the quaterthiophene part. It is likely that such a quaterthiophene moiety with an extended π-conjugation is able to be oxidized at lower potentials.

EL characteristics of the OLEDs

Fig. 3 illustrates EL characteristics of the five types of devices. As the device structures change, both current–voltage (*I–V*) and luminance–voltage (*L–V*) curves of these devices shift to higher voltages in the order of SAM(**2**) < SAM(**1**) ~ bare-ITO < bare-Au < SAM(**3**). Compared with the bare-Au device, the *I–V* and *L–V* curves of the SAM(**1**) and SAM(**2**) devices shift to a low voltage direction by about 1 V and 3 V, respectively. The operating voltage at a luminance of 100 cd m^{-2} decreases from 9.5 V for the bare-Au device to 8.5 V for the SAM(**1**) device and to 6.3 V for the SAM(**2**) device. This large reduction in operating voltage is related to the combination of a tripod-shaped head-group and a large π-conjugated system in the molecules of **1** and **2**. Unlike the SAM(**1**) and SAM(**2**) devices, the *I–V* and *L–V* curves of the SAM(**3**) device shift to high voltages. The operating voltage of the SAM(**3**) device at a luminance of 100 cd m^{-2} increases up to 11.4 V. The relative positions of the *I–V* curves for these devices demonstrate that the hole injection is enhanced by using the Au coated with SAM **1** or SAM **2** as an anode compared with the bare-Au anode, but depressed by using SAM **3**.

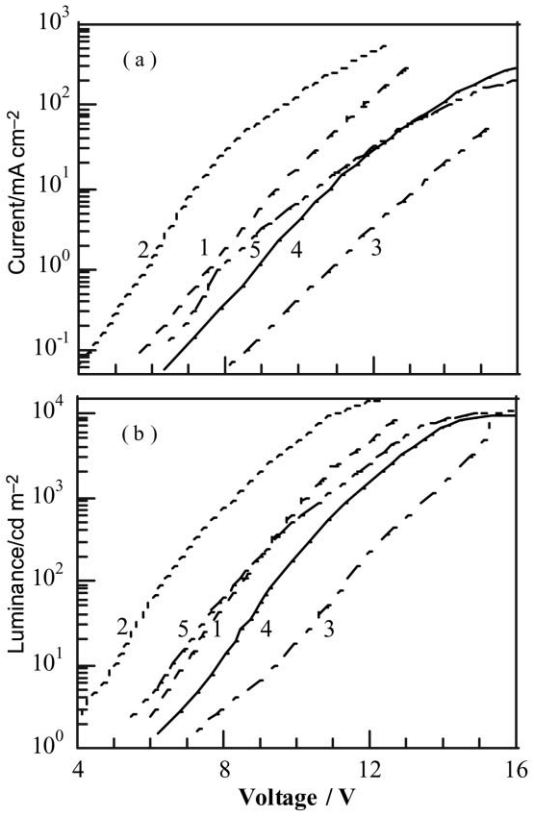

Fig. 3 *I–V* (a) and *L–V* (b) characteristics of (1) SAM(**1**), (2) SAM(**2**), (3) SAM(**3**), (4) bare-Au, and (5) bare-ITO devices.

It is also known from Fig. 3 that the SAM(**1**) and SAM(**2**) devices exhibit maximum current densities of 320 and 455 mA cm^{-2}, much greater than that of the SAM(**3**) device (64 mA cm^{-2}). This hints that SAMs **1** and **2** are quite stable, whereas SAM **3** has a poor stability, being consistent with the electrochemical stability of these SAMs estimated from the cyclic voltammetric measurements. The different stability of these SAMs also accounts for the different maximum brightnesses, *i.e.*, 9200, 14000 and 6800 cd m^{-2} for SAM(**1**), SAM(**2**), and SAM(**3**) devices, respectively.

In addition, it is noted in Fig. 3 that the *I–V* and *L–V* curves of the bare-ITO device lie on the right side of those of the bare-Au device. The operating voltage of the bare-ITO device at a luminance of 100 cd m^{-2} is 8.5 V, lower than 9.5 V for the bare-Au device. It is somewhat in contradiction with the expectation that the operating voltage of the bare-Au device should be lower than that of the bare-ITO device because bare Au substrate has a work function of 5.1 eV, greater than 4.7 eV for the ITO substrate. The transparency of the Au/mica substrate used in the present work was measured to be about 30% in the visible region. The operating voltage of the bare-Au device will be reduced to an extent when the transparency is corrected. However, the contradiction is still difficult to explain with a simple energy diagram model for OLEDs (see the discussion later).

Possible reasons of the SAMs' effects on the operating voltages of the OLEDs

The results shown in Fig. 3 clearly indicate that the operating voltages of the OLEDs can be tuned by the SAMs. The different influences of SAMs **1**–**3** on the operating voltages of the devices can be explained by considering the structures of the thiol and disulfide molecules and SAMs, and the energy level alignment at the related interfaces in the devices.

The symmetry of tripod-shaped molecules with a rigid π-conjugated oligothiophene tail favors the molecules to stand up almost normal to the Au/mica surface. This facilitates charge transport from the Au anode through the SAM **1** or SAM **2** layer to the TPD layer. In contrast, the two arms of quaterthiophene in the molecule of **3** cannot stand up in such a way if the S–S bond is not cleaved in SAM **3**. These structural differences are consistent with the low surface coverage of SAM **3** and with the more positive oxidation potential of **3** than **2** (Fig. 2). The enhanced charge transfer from the Au anode to the TPD layer by coating with SAMs **1** and **2** leads to a markedly reduced operating voltage of the corresponding devices. This kind of reduced operating voltage cannot be achieved in the SAM(**3**) device due to the poorer charge transfer through the SAM **3** layer.

Fig. 4 gives schematic energy diagrams for the devices with and without the SAMs. The hole injection barrier for the

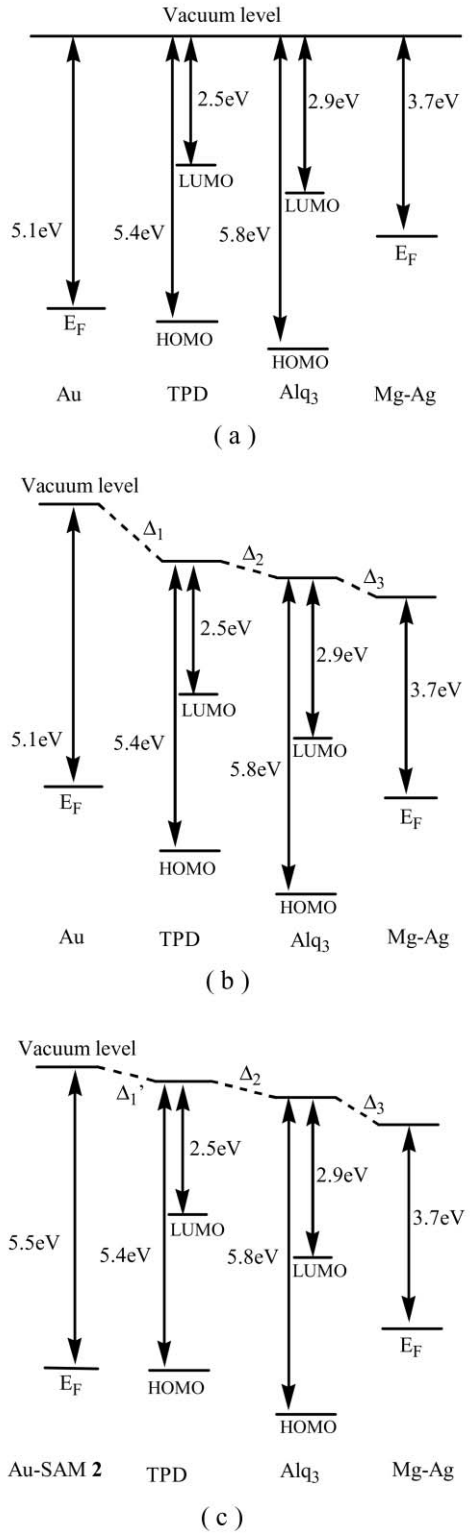

Fig. 4 Schematic energy diagrams of EL devices with (a) and (b) bare Au electrode and (c) SAM **2**-coated Au electrode as anode.

bare-Au device is dependent on the difference between the work function of Au and the HOMO energy of TPD, the adhesion of the TPD layer, and some other factors. The roles of SAMs in the related EL devices become clearer by considering the influences of the SAMs on the vacuum level shift for the interface between Au and TPD in the energy diagrams (Fig. 4c).

For the bare-Au device (Fig. 4a), the work function of Au (Φ_m) is not much different from the ionization potential (I_p) or the HOMO energy of TPD. This small difference suggests a small hole injection barrier, which is in contradiction with the poor *I–V* property of the bare-Au device (Fig. 3a). This small barrier is based on the Mott-Schottky model,[15] where the vacuum level of an organic semiconductor is assumed to coincide with that of a metal substrate at the interface. This assumption of the alignment of the vacuum levels at the metal/organic or organic/organic interfaces has been recently shown to be in general invalid under open-circuit conditions.[15–17] At these interfaces, in fact, the vacuum levels of organic material and metal do not align at the interface, due to the formation of an electric dipole layer at the interface. Such a potential difference between outermost metal surface and first organic layer is defined as vacuum level shift (Δ), corresponding to the failure of the Mott-Schottky model. The polarity of the vacuum level shift is often negative, and the value of this shift depends on both the metal and organic materials.

The vacuum level shifts at the Au/TPD, TPD/Alq_3 and Alq_3/Mg–Ag interfaces in Fig. 4b are referred to as Δ_1, Δ_2, and Δ_3, respectively. It should be noted that Mg, being one of reactive metals, is found to diffuse rapidly into Alq_3, when deposited on the organic layer, leading to a broad doped interface.[18] Such a diffusion of Mg induces new electronic gap states. Thus, unlike Δ_1 and Δ_2, Δ_3 includes both the interface dipole barrier (0.15 eV) and the doping-induced molecular level shift (0.5 eV).[18] However, it is unnecessary to consider the exact value of Δ_3 in the present work because the organic heterojunctions in the cathode side are the same for all of the tested devices. The barrier height for hole injection should be estimated as $|I_p - \Phi_m - \Delta_1|$, where Δ_1 is the vacuum level shift at the metal/TPD interface. The values of the vacuum level shift are reported as about -1.15 eV for the Au/TPD interface[15] and -0.3 eV for ITO/TPD interface.[16] As demonstrated in Fig. 3a, the *I–V* property of the bare-Au device is poorer than that of the bare-ITO device, although the work function of ITO is about 4.7 eV, being smaller than that (5.1 eV) of Au. This apparent contradiction comes from the quite different values of the vacuum level shift for the ITO/TPD and Au/TPD interfaces.

When the SAM-coated Au electrode is used as the anode instead of the bare-Au electrode, the situation changes at the anode/TPD interface, because the work function of Au(111) surface is apparently affected by the SAM. By using the Kelvin probe method,[19] we found that the work function of the SAM-coated Au(111) in air was 5.3 eV for SAM **1** and 5.5 eV for SAM **2**, whereas the value in the case of SAM **3** was roughly the same as 5.1 eV for the bare Au surface. The energy diagram of the device using SAM **2**-coated Au as an anode is illustrated in Fig. 4c. The vacuum level shift has been suggested to occur between the outermost metal surface and the first organic layer, and the shift at an organic/organic interface is often small, compared to that at metal/organic interface. For instance, the band offset between Au and TPD is -1.15 eV, whereas the band offset between Alq_3 and TPD is only about -0.13 eV.[20] In the SAM(**2**) device, the SAM **2** is compact on Au(111)/mica substrates, the TPD layer directly contacts the (organic) SAM **2** and does not contact the (metallic) Au. It is rational to assume that the band offset at Au-SAM **2**/TPD interface ($|\Delta_1'|$) is much smaller than $|\Delta_1| \approx 1.1$ eV. As a consequence, the hole injection barrier height at the anode becomes very small, being reduced markedly in comparison with 1.4 eV for the bare-Au device. This results in considerably reduced operating voltages of the SAM(**2**) device. A similar situation occurs also in the SAM(**1**) device, although the reduction in the operating voltage is less due to the somewhat poorer compactness of SAM **1**.

The poor EL characteristic of the SAM(**3**) device is directly related to the poor compactness of SAM **3**, as indicated by its low surface coverage. The Au surface coated with SAM **3** may be considered as being partially metallic and partially organic due to this small surface coverage. Thus, it is assumed that the absolute value of the band offset at the Au-SAM **3**/TPD interface ($|\Delta_1''|$) increases to a value considerably greater than

that at the Au-SAM **2**/TPD interface ($|\Delta_1'|$). In other words, the band offset at the Au-SAM **3**/TPD interface is great compared with that at the Au-SAM **2**/TPD interface. This is at least partly consistent with the fact that the coating of SAM **3** does not evidently change the value of the work function of Au. These may lead to increase of the hole injection barrier height in the SAM(**3**) device, resulting in higher operating voltages.

Conclusions

SAMs of two tripod-shaped oligothiophene-bearing thiols and a disulfide have been grafted on a Au(111) surface. Electrochemical measurements indicate that the packing within the SAM of the tripod-shaped thiol **2** is compact, that within the SAM of thiol **1** less so, whilst that within the SAM of disulfide **3** is very poor. Because of the different molecular structures and the different packing within the SAMs, the electrochemical oxidation/reduction behaviors resulting from the π-conjugated oligothiophene moieties are quite different for each of these SAMs. Electrochemical oxidation of SAM **1** takes place easily and is reversible, and the three-point anchors in the molecules of **1** result in good stability of its SAM. These features strongly suggest that SAM **1** can facilitate charge transport. However, both the much increased tail length of the molecule of **1** and the higher number of C_6H_{13} substituents cause its SAM to be less compact than that of **2**, and make a perfect standing of the molecules on the Au surface difficult. These are unfavorable factors for charge transport through the SAM. In the case of **2**, the π-conjugated tail has an appropriate length, allowing compact packing of the molecules. Thus, the charge transport will be greatly enhanced by SAM **2**. The SAM-coated Au(111) electrodes have been used to fabricate EL devices. Compared to the bare-Au device, the SAM **2** device exhibits significantly improved EL performance, for instance, greatly-reduced operating potentials, yielding much greater maximum brightness, permitting much higher currents, and better stability. The enhancing effect of SAM **2** on the EL performance of the device is closely related to its tripod-shaped structure. In contrast, the SAM(**3**) device shows EL characteristics poorer than the bare-Au device. The different effects of the SAMs on the EL properties of the devices have also been discussed by considering the modifications of the surface potential of Au and the vacuum level shift at the Au/TPD interface by the SAMs. These modifications influence the hole injection barrier height at the anode/TPD interface and hence affect the EL characteristics of the devices.

References

1 J. Kido (Editor), *Organic Electroluminescence Materials and Displays*, CMC Inc., Tokyo, 2001.
2 S. A. VanSlyke, C. H. Chen and C. W. Tang, *Appl. Phys. Lett.*, 1996, **69**, 2160.
3 L. Zhu, H. Tang, Y. Harima, Y. Kunugi, K. Yamashita, J. Ohshita and A. Kunai, *Thin Solid Films*, 2001, **273**, 214.
4 L. Zhu, H. Tang, Y. Harima, K. Yamashita, J. Ohshita and A. Kunai, *Synth. Met.*, 2002, **126**, 333.
5 F. Schreiber, *Prog. Surf. Sci.*, 2000, **65**, 151.
6 I. H. Campbell, S. Rubin, T. A. Zawodzinski, J. D. Kress, R. L. Martin, D. L. Smith, N. N. Barashkov and J. P. Ferraris, *Phys. Rev. B*, 1996, **54**, R14321.
7 I. H. Campbell, J. D. Kress, R. L. Martin, D. L. Smith, N. N. Barashkov and J. P. Ferraris, *Appl. Phys. Lett.*, 1997, **71**, 3528.
8 F. Nüesch, F. Rotzinger, L. Si-Ahmed and L. Zuppiroli, *Chem. Phys. Lett.*, 1998, **288**, 861.
9 S. F. J. Appleyard and M. R. Willis, *Opt. Mater.*, 1998, **9**, 120.
10 C. Ganzorig, K.-J. Kwak, K. Yagi and M. Fujihira, *Appl. Phys. Lett.*, 2001, **79**, 272.
11 L. Zhu, H. Tang, Y. Harima, K. Yamashita, D. Hiroyama, Y. Aso and T. Otsubo, *Chem. Commun.*, 2001, 1830.
12 D. Hirayama, K. Takimiya, Y. Aso, T. Otsubo, T. Hasobe, H. Yamada, H. Imahori, S. Fukuzumi and Y. Sakata, *J. Am. Chem. Soc.*, 2002, **124**, 532.
13 C. A. Widrig, C. Chung and M. D. Porter, *J. Electroanal. Chem.*, 1991, **310**, 335.
14 L. Zhu, H. Tang, Y. Harima, K. Yamashita, J. Ohshita and A. Kunai, *J. Appl. Electrochem.*, 2001, **31**, 175 and references therein.
15 H. Ishii, H. Oji, E. Ito, N. Hayashi, D. Yoshimura and K. Seki, *J. Lumin.*, 2000, **87-89**, 61 and references therein.
16 H. Peisert, T. Schwieger, K. Knupfer, M. S. Golden and J. Fink, *J. Appl. Phys.*, 2000, **88**, 1535.
17 R. Treusch, F. J. Himpsel, S. Kakar, L. J. Terminello, C. Heske, T. van Buuren, V. V. Dinh, H. W. Lee, K. Parkbaz, G. Fox and I. Jiménez, *J. Appl. Phys.*, 1999, **86**, 88.
18 A. Rajagopal and A. Kahn, *J. Appl. Phys.*, 1998, **84**, 355.
19 Y. Harima, K. Yamashita, H. Ishii and K. Seki, *Thin Solid Films*, 2000, **366**, 237.
20 R. Schlaf, B. A. Parkinson, P. A. Lee, K. W. Nebesny and N. R. Armstrong, *Appl. Phys. Lett.*, 1998, **73**, 1026.